AT-cut quartz plate, or on Mylar for transmission. It is essential to rotate the specimen and increase the count time. A Gandolfi camera has also been used for very small specimens (see Section 2.3.4). A high-brilliance microfocus X-ray source has been used with a collimator made of 10 to 100 μm internal-diameter capillary tube. An *X*–*Y* stage is used with an optical microscope to locate selected areas of the specimen.

A microdiffractometer has been designed for microanalysis, Fig. 2.3.1.15 (Rigaku Corporation, 1990). It has been used to determine phases and stress in areas $< 10^4\ \mu m^2$ (Goldsmith & Walker, 1984). The key to the method is the use of an annular-ring receiving slit, which transmits the entire diffraction cone to the detector instead of a small chord as in conventional diffractometry, thereby utilizing all the available intensity. The pattern is scanned by translating the ring and detector along the direct-beam path so that

$$2\theta = \arctan(R_{RS}/L), \qquad (2.3.1.26)$$

where R_{RS} is the radius of the ring slit and L the distance from the fixed specimen. For $R_{RS} = 15$ mm, L varies from 171 to 9 mm in the transmission range 5 to 60°2θ; a 50 mm diameter scintillation counter is used. A doughnut-shaped proportional counter (3/4 of a full circle) is used for the 30 to 150° reflection specimen mode. The slit width is 0.2 mm and the aperture varies with 2θ. The intensities fall off at the higher 2θ's because of the small incidence angles to the slit. An alternative method uses a position-sensitive proportional counter. Steinmeyer (1986) has described applications of microdiffractometry.

By using synchrotron radiation (Section 2.3.2), single-crystal data for structure determination can now be obtained from a microcrystal about 5–10 μm in size; see Andrews *et al.* (1988), Bachmann, Kohler, Schultz & Weber (1985), Harding (1988), Newsam, King & Liang (1989), Cheetham, Harding, Mingos & Powell (1993), Harding & Kariuki (1994), and Harding, Kariuki, Cernik & Cressey (1994).

2.3.2. Parallel-beam geometries, synchrotron radiation

The radiation from the X-ray tube is divergent and various methods can be used to obtain a parallel beam as shown in Fig. 2.3.2.1. Symmetrical reflection from a flat crystal is the usual method. An asymmetric reflecting monochromator with small incidence angle and large exit angle expands the beam, or in reverse condenses it (§2.3.5.4.1). A channel monochromator has the advantage of not changing the beam direction. A receiving slit or preferably Soller slits can be used to define the diffracted beam. A graphite monochromator in the diffracted beam or a solid-state detector eliminates fluorescence. The incident-beam parallel slits limit vertical divergence. However, all the methods result in a large loss of intensity compared with conventional focusing. In contrast, the storage ring produces a virtually parallel beam with very small vertical divergence of about 0.1 mrad, and the monochromator is used only to select the wavelength. The rest of this section assumes a synchrotron-radiation source.

Storage-ring X-ray sources have a number of unique properties that are of great importance for powder diffraction. The advantages of synchrotron powder diffraction have been described by Hastings, Thomlinson & Cox (1984), Parrish & Hart (1987), Parrish (1988), and Finger (1989). Excellent patterns with high resolution and high peak-to-back ground ratio have been reported. These include the orders-of-magnitude higher intensity and nearly uniform spectral distribution compared with X-ray tubes, the wide continuous range of selectable wavelengths, and the single profile that avoids the problems caused by $K\alpha$ doublets and β filters. Owing to major differences in the diffractometer geometries, comparisons of intensities with X-ray tube focusing methods cannot be predicted simply from the number of source photons.

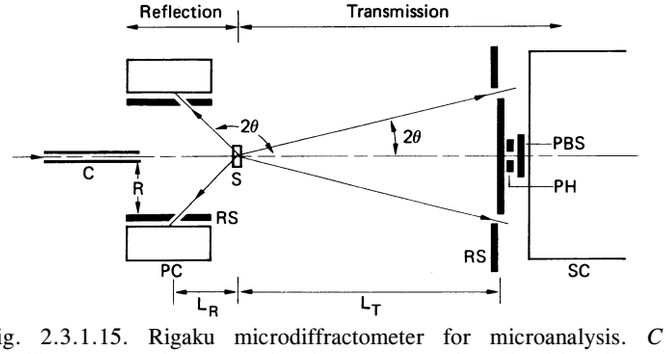

Fig. 2.3.1.15. Rigaku microdiffractometer for microanalysis. *C* collimator, PC ring proportional counter, RS ring slit with radius *r*, *S* specimen, SC scintillation counter, PBS primary beam stop, PH pinhole for alignment, *L* specimen-to-receiving-slit distance.

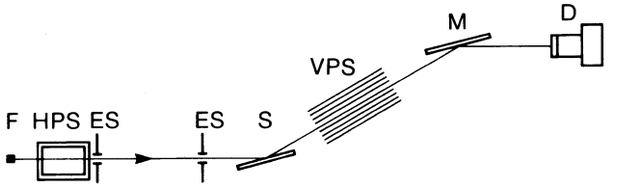

Fig. 2.3.2.1. Method to obtain parallel beam from X-ray tube for powder diffraction. HPS parallel slits to limit axial divergence, ES entrance slits (can be replaced by pair of flat parallel steel bars), *S* specimen, VPS parallel slits to define diffracted beam, *M* flat monochromator (can be omitted). *D* detector. See also Fig. 2.3.2.4(*a*).

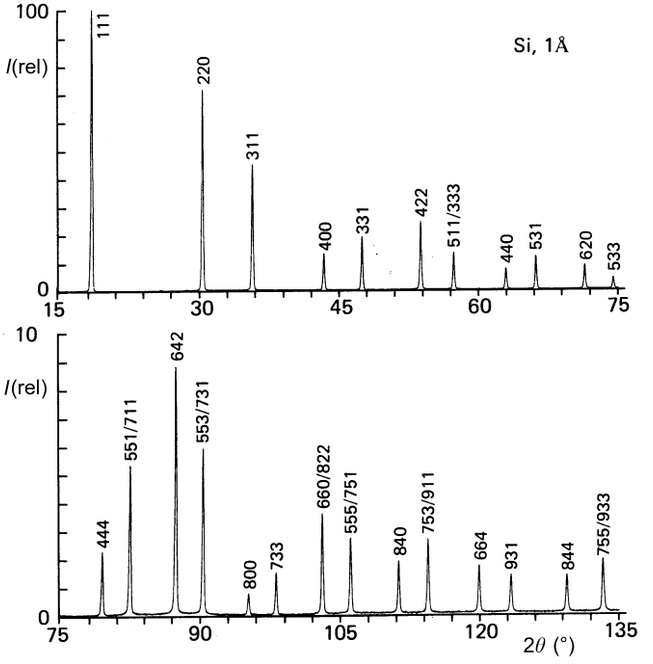

Fig. 2.3.2.2. Silicon powder pattern with 1 Å synchrotron radiation using method shown in Fig. 2.3.2.4(*a*). The 444 reflection is the limit for Cu $K\alpha$ radiation.

The easy wavelength selection makes it possible to avoid specimen fluorescence, to record data on both sides of an absorption edge for anomalous-scattering studies, to select optimum angles and wavelengths for lattice-parameter measurements, and to vary the dispersion. Short-wavelength radiation can be used for uncomplicated patterns without the background occurring in X-ray tube spectra. Fig. 2.3.2.2 shows a silicon pattern obtained with 1.0 Å X-rays in which there are twice as many reflections as can be recorded with Cu $K\alpha$, and the background remains very low out to the highest 2θ angles. The short wavelengths (~ 0.7 Å) are especially useful for samples mounted in cryostats, furnaces, and pressure cells.

Using an incident-beam tunable monochromator, no continuous radiation reaches the specimen and a wavelength can be selected that gives a high peak-to-background ratio and no specimen fluorescence. If the specimen contains different chemical phases, patterns can be recorded using wavelengths on both sides of the absorption edge to enhance one of the patterns as an aid in identification. This is illustrated in Fig. 2.3.2.3 for a mixture of Ni and ZnO powders. A pattern (*a*) with maximum peak-to-background ratio is obtained with a wavelength slightly longer than the Ni *K*-absorption edge but using a wavelength shorter than the edge (*b*) causes high Ni *K* fluorescence background. The relative intensities of the peaks in each compound are the same with both wavelengths. However, the large change in the Ni absorption across the edge caused a large difference in the ratio of Ni/ZnO intensities. The Ni(111) decreased by 85% and the intensity ratio Ni(111)/ZnO(102) dropped from 4.2 to 1.3.

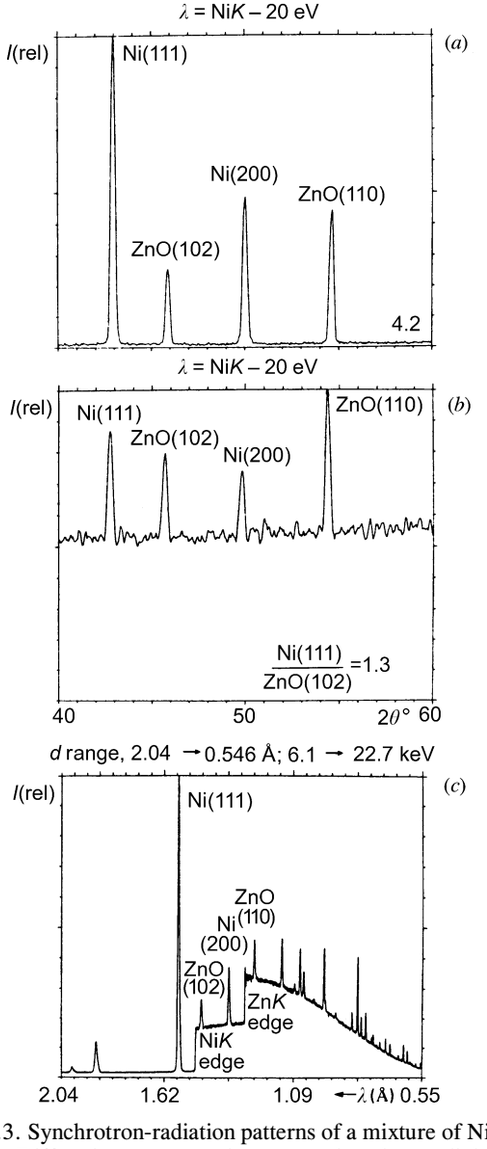

Fig. 2.3.2.3. Synchrotron-radiation patterns of a mixture of Ni and ZnO powders. Diffraction pattern using a wavelength (*a*) slightly longer than the Ni *K*-absorption edge and (*b*) slightly shorter. (*c*) High-resolution energy-dispersive diffraction (EDD) pattern.

Modified conventional vertical-scanning diffractometers are used to avoid intensity losses from the strong polarization in the horizontal plane. The six basic powder diffraction methods that have been used are:

(*a*) Monochromatic X-rays with θ–2θ scanning and flat specimen as in conventional X-ray tube methods but using parallel-beam X-ray optics. This is the most widely applicable method for polycrystalline materials.

(*b*) Monochromatic X-rays with fixed specimen and 2θ detector scan, used for analysing texture, preferred orientation, and grazing-incidence diffraction.

(*c*) Monochromatic X-rays with a capillary specimen and scanning receiving slit or position-sensitive detector.

(*d*) Energy-dispersive diffraction using a step-scanned channel monochromator, selectable fixed θ–2θ positions, and conventional scintillation counter and electronics. The instrumentation is the same as (*a*) and may be used in methods that require a stationary specimen.

(*e*) Energy-dispersive diffraction using the white beam, solid-state detector and multichannel analyser, and selected fixed θ–2θ. This is the method frequently used with synchrotron and X-ray tube sources but it has low pattern resolution (Giessen & Gordon, 1968).

(*f*) Angle-dispersive or energy-dispersive experiments with an imaging-plate detector, whereby complete Debye–Scherrer rings are recorded simultaneously, as in some film methods (Subsection 2.3.4.1) (*e.g.* Piltz *et al.*, 1992). This is a particularly useful technique for studies under non-ambient conditions, such as experiments at ultra-high pressure (*e.g.* McMahon & Nelmes, 1993).

2.3.2.1. *Monochromatic radiation, θ–2θ scan*

The X-ray optics of a plane-wave parallel-beam diffractometer is shown schematically in Fig. 2.3.2.4(*a*). The primary white beam is limited by slits at *C*1. A channel monochromator CM is used because it has the important property of maintaining the same direction and position for a wide range of wavelengths. It may be used in the dispersive setting with respect to the specimen or in the parallel setting [Fig. 2.3.2.4(*b*)]. The monochromatic beam is larger than the entrance slit ES and it is unnecessary to realign the powder diffractometer when changing wavelengths. The monochromator can be mounted on a stripped diffractometer for easy alignment and step scanning.

There are no characteristic spectral lines and the wavelength calibration of the monochromator is made by step scanning the monochromator across absorption edges of elements in a specimen or pure element foils placed in the beam. The wavelength accuracy is limited by the uncertainty as to what feature of the edge should be measured and which one was used for the wavelength tables. A standard powder sample such as NIST silicon 640b whose lattice parameter is known with moderately high precision can also be used. An alternative method is to measure the reflection angle of a single-crystal plate of float-zones oxygen-free silicon whose lattice parameter is known to 1 part in 10^{-7} and to determine the wavelength from

the Bragg equation (Hart, 1981). The accuracy is then limited by the angular accuracy of the diffractometer and the orientation setting.

It is necessary to monitor the monochromatic beam intensity I_0, which changes during the recording due to decreasing storage-ring current, orbital shifts or other factors. This can be done by inserting a low-absorbing ionization chamber in the beam or by using a scintillation counter to measure scattering from an inclined thin beryllium foil, kapton or other low-absorbing material. The data are recorded and used to correct the observed intensities. The monitored counts can also be used as a timer for step scanning if a sufficient number are recorded for good counting statistics.

The entrance slit ES determines the irradiated specimen length, which is equal to ES/sin θ_s. Vertical parallel slits VPS with $\delta \simeq 2^\circ$ are used to limit the axial divergence. The longer the distance between the specimen and detector, the smaller the asymmetry, and a vacuum path should be used to avoid air-absorption losses. The specimen may be used in either reflection or transmission simply by rotating it 90° around the diffractometer axis from its previous position.

The diffracted beam can be defined by a receiving slit (Parrish, Hart & Huang, 1986), horizontal parallel slits HPS [Fig. 2.3.2.4(*a*)] (Parrish & Hart, 1985) or a high-quality single-crystal plate which acts as a very narrow receiving slit [Fig. 2.3.2.4(*b*)] (Cox, Hastings, Thomlinson & Prewitt, 1983; Hastings *et al.*, 1984). If a receiving slit is used, the intensity, profile width and shape are determined by the widths of both ES and RS. If either one is much wider than the other, the profile has a flat top. Increasing the RS width and keeping ES constant causes symmetrical profile broadening and increases the intensity as in conventional focusing diffractometry. There are disadvantages in using a receiving slit because the intensities are low and it causes the same specimen-surface-displacement and transparency errors as the focusing geometries.

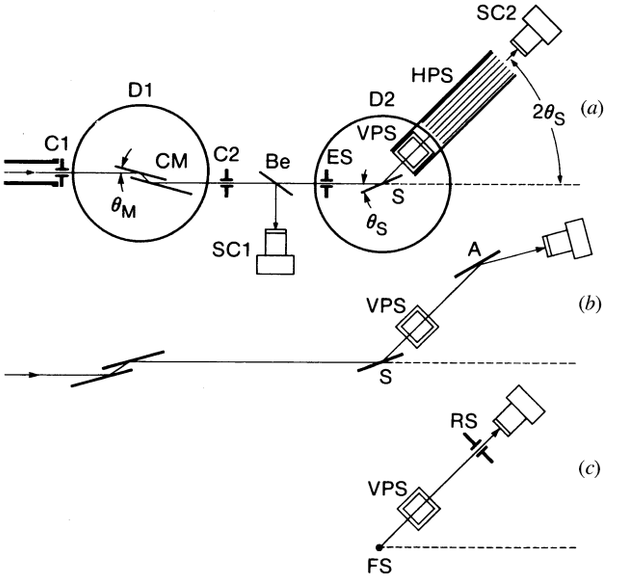

Fig. 2.3.2.4. (*a*) Optics of dispersive parallel-beam method for synchrotron X-rays. *C*1 primary-beam collimator, *D*1 diffractometer for channel monochromator CM, *C*2 antiscatter shield, Be beryllium foil for monitor, SC1 and SC2 scintillation counters, ES entrance slit on powder diffractometer *D*2, VPS vertical parallel slits to limit axial divergence, HPS horizontal parallel slits, which determine the resolution. (*b*) CM in nondispersive setting and crystal analyser *A* used as a narrow receiving slit. (*c*) Fibre specimen FS with receiving slit RS or with position-sensitive detector (not shown) with RS removed.

A set of horizontal parallel (Soller) slits is advantageous because of the much higher intensity and it eliminates the displacement errors. The profiles of specimens without broadening effects have the same FWHM as the aperture of the slits, equation (2.3.1.7). The FWHM increases as $\tan\theta$ due to wavelength dispersion. By increasing the length of the foils and keeping the same spacing, the aperture can be reduced to increase the resolution without large loss of intensity. A set of 365 mm long slits with 0.05° aperture has been used and even smaller apertures are feasible. Longer slits decrease the fluorescence intensity (if any) reaching the detector. They must be carefully made and aligned to avoid loss of intensity and should be evacuated or filled with He to avoid air-absorption losses.

The use of a crystal analyser eliminates fluorescence and gives the highest resolution powder profiles with FWHM = 0.02 to 0.05°2θ, depending on the quality of the crystal (Hastings *et al.*, 1984). The alignment of the crystal is critical and must be done with remote automated control every time the wavelength is changed. Displacement aberrations are eliminated but the intensity is much lower than the HPS because of the small rocking angle and low integrated reflectivity of the crystal.

The correct orientation of crystalline powder particles for reflection is far more restrictive for the parallel beam than the X-ray tube divergent beam. A much smaller number of particles will have the exact orientation for reflection, and thus the recorded intensity will be lower and relative intensities less accurate. If the specimen is stationary, the standard deviations of the intensities due to particle size are six to nine times higher than in focusing methods (Parrish, Hart & Huang, 1986). It also becomes more difficult to achieve the completely randomly oriented specimens required for structure determination and quantitative analysis and, as in X-ray tube data, a preferred-orientation term is included in the structure refinement. It is, therefore, essential to use small particles $< 10\,\mu$m and to rotate the specimen. Some investigators prefer to oscillate the specimen over a small angle but this is not as effective as rotation.

The profiles are virtually symmetrical except at small angles where axial divergence causes asymmetry. The profiles in Fig. 2.3.2.5 show the differences in the shape and resolution obtained with conventional focusing (*a*) and parallel-beam synchrotron methods (*b*). The effect of the higher resolution on a mixture of nearly equal volumes of quartz, orthoclase, and feldspar recorded with X-ray tube focusing methods is shown in Fig. 2.3.2.5(*c*) and with synchrotron radiation in Fig. 2.3.2.5(*d*). The symmetry and nearly constant simple instrument function make it easier to separate overlapping reflections and simplify the profile-fitting procedures and the interpretation of specimen-broadening effects.

The early crystal-structure studies using Rietveld refinement were not as successful with X-ray tube focusing methods as they were with neutron diffraction because the complicated instrument function made profile fitting difficult and inaccurate. The development of synchrotron powder methods with simple symmetrical instrument function, high resolution, and the use of longer wavelengths to increase the dispersion have made structural studies as successful as with neutrons, and have the advantage of orders-of-magnitude higher intensity. Some examples are described by Attfield, Cheetham, Cox & Sleight (1988), Lehmann, Christensen, Fjellvåg, Feidenhans'l & Nielsen (1987), and *ab initio* structure determinations by

McCusker (1988), Cernik *et al.* (1991), Morris, Harrison, Nicol, Wilkinson & Cheetham (1992), and others.

Structures have also been solved using a two-stage method in which the integrated intensities are determined by profile fitting the individual reflections and used in a powder least-squares refinement method (*POWLS*) (Will, Bellotto, Parrish & Hart, 1988). The method was tested with silicon, which gave R(Bragg) 0.7%, and quartz, which gave 1.6%, which is a good test of the high quality of the experimental data and the profile-fitting procedure. Fig. 2.3.2.6 shows Fourier maps of orthorhombic Mg_2GeO_4 calculated using Fourier coefficients taken directly from the profile-fitting intensities.

Other types of powder studies have been carried out successfully. For example, these have been used in anomalous-scattering studies (Will, Masciocchi, Hart & Parrish, 1987; Will, Masciocchi, Parrish & Hart, 1987), Warren–Averbach profile-broadening analysis (Huang, Hart, Parrish & Masciocchi, 1987), studies of texture in thin films (Hart, Parrish & Masciocchi, 1987), and precision lattice-parameter determination (Hart, Cernik, Parrish & Toraya, 1990).

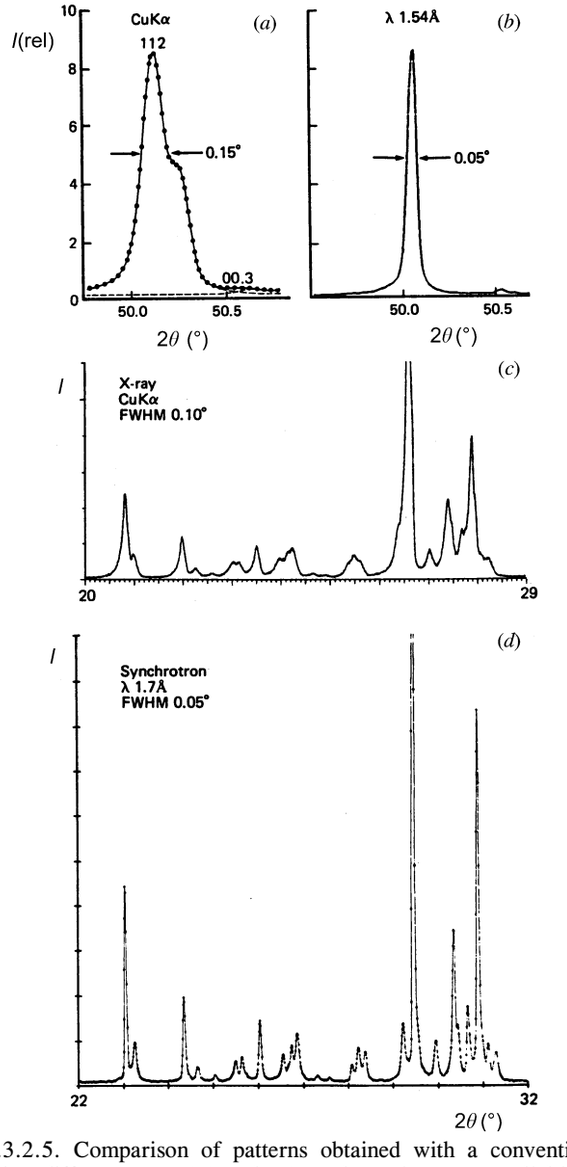

Fig. 2.3.2.5. Comparison of patterns obtained with a conventional focusing diffractometer (*a*) and (*c*), and synchrotron parallel-beam method (*b*) and (*d*). (*a*) and (*b*) quartz powder profiles; (*c*) and (*d*) mixture of equal amounts of quartz, orthoclase, and feldspar.

2.3.2.2. *Cylindrical specimen, 2θ scan*

The flat specimen can be replaced by a thin cylindrical [Fig. 2.3.2.4(*c*)] specimen as used in powder cameras. The powder can be coated on a thin fibre or reactive materials can be forced into a capillary to avoid contact with air. The intensity is lower than for flat specimens because of the smaller beam, and less powder is required. Thompson, Cox & Hastings (1987) used the method to determine the structure of Al_2O_3 by Rietveld refinement. They used a two-crystal incident-beam Si(111) monochromator; the first crystal was flat and the second a cylindrically bent triangular plate for sagittal focusing to form a 4×2 mm beam with spectral bandwidth $\Delta\lambda/\lambda \simeq 10^{-3}$.

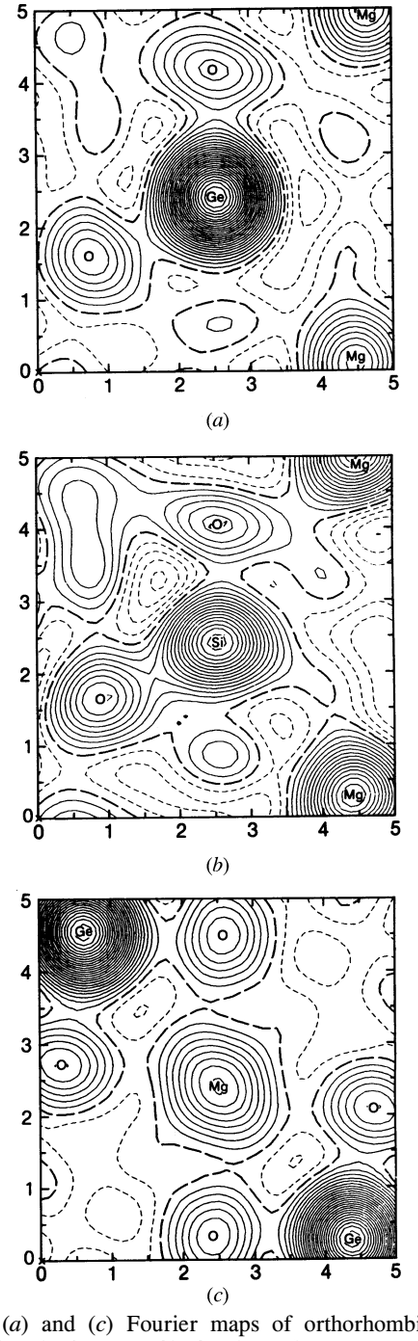

Fig. 2.3.2.6. (*a*) and (*c*) Fourier maps of orthorhombic Mg_2GeO_4 calculated directly from profile-fitted synchrotron powder data. (*b*) Fourier section of isostructural Mg_2SiO_4 calculated from single-crystal data for comparison with (*a*).

The method can also be used with a receiving slit or position-sensitive detectors (Lehmann *et al.*, 1987; Shishiguchi, Minato & Hashizume, 1986). The latter can be a short straight detector, which can be scanned to increase the data-collection speed (Göbel, 1982), or a longer curved detector.

2.3.2.3. *Grazing-incidence diffraction*

In conventional focusing geometry, the specimen and detector are coupled in θ–2θ relation at all 2θ's to avoid defocusing and profile broadening. In Seemann–Bohlin geometry, changing the specimen position necessitates realigning the diffractometer and very small incidence angles are inaccessible. In parallel-beam geometry, the specimen and detector positions can be uncoupled without loss of resolution. This freedom makes possible the use of different geometries for new applications. The specimen can be set at any angle from grazing incidence to slightly less than 2θ, and the detector scanned. Because the incident and exit angles are unequal, the relative intensities may differ by small amounts from those of the θ–2θ scan due to specimen absorption. The reflections occur from differently oriented crystallites whose planes are inclined (rather than parallel) to the specimen surface so that particle statistics becomes an important factor. The method is thus similar to Seemann–Bohlin but without focusing.

The method can be used for depth-profiling analysis of polycrystalline thin films using grazing-incidence diffraction (GID) (Lim, Parrish, Ortiz, Bellotto & Hart, 1987). If the angle of incidence θ_i is less than the critical angle of total reflection θ_c, diffraction occurs only from the top 35 to 60 Å of the film. Comparison of the GID pattern with a conventional θ–2θ pattern in which the penetration is much greater gives structural information for phase identification as a function of film depth. The intrinsic profile shapes are the same in the two patterns and broadening may indicate smaller particle sizes. However, if the film is epitaxic or highly oriented, it may not be possible to obtain a GID pattern.

For $\theta_i < \theta_c$, the penetration depth t' is (Vineyard, 1982)

$$t' \simeq \lambda/[2\pi(\theta_c^2 - \theta_i^2)^{1/2}] \qquad (2.3.2.1)$$

and, for $\theta_i > \theta_c$,

$$t' \simeq 2\theta_i/\mu, \qquad (2.3.2.2)$$

where μ is the linear absorption coefficient. The thinnest top layer of the film that can be sampled is determined by the film density, which may be less than the bulk value. As θ_i approaches θ_c, the penetration depth increases rapidly and fine control becomes more difficult. Fig. 2.3.2.7 shows this relation and the advantage of using longer wavelengths for a wider range of penetration control. For example, for a film with $\mu = 200\,\text{cm}^{-1}$, $\lambda = 1.75$ Å, and $\theta_i = 0.1°$, only the top 45 Å contribute, and increasing θ_i to 0.35° increases the depth to 130 Å. The patterns have much lower intensity than a θ–2θ scan because of the smaller diffracting volume.

Fig. 2.3.2.8 shows patterns of a 5000 Å polycrystalline film of iron oxide deposited on a glass substrate and recorded with (*a*) θ–2θ scanning and (*b*) 0.25° GID. The film has preferred orientation as shown by the numbers above the peaks in (*a*), which are the relative intensities of a random powder sample. The relative intensities are different because in (*a*) they come from planes oriented parallel to the surface and in (*b*) the planes are inclined. The glass scattering that is prominent in (*a*) is absent in (*b*) because the beam does not penetrate to the substrate.

2.3.2.4. *High-resolution energy-dispersive diffraction*

By step scanning the channel monochromator instead of the specimen, a different wavelength reaches the specimen at each step and the pattern is a plot of intensity *versus* wavelength or energy (Parrish & Hart, 1985, 1987). The X-ray optics can be the same as described in Subsection 2.3.2.1 and determines the resolution. A scintillation counter with conventional electronic circuits can be used. As in the conventional white-beam energy-

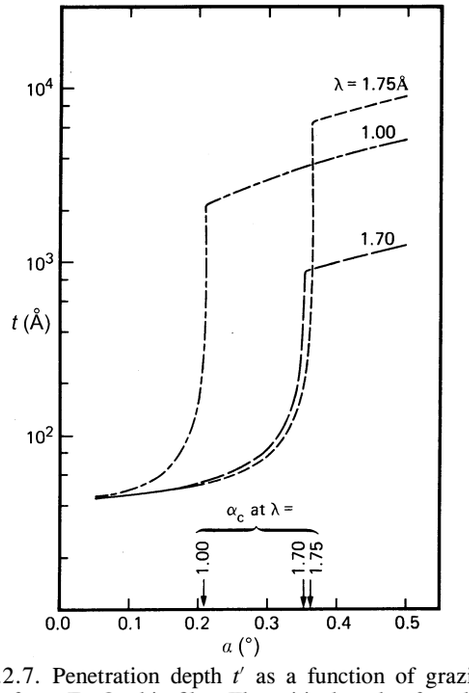

Fig. 2.3.2.7. Penetration depth t' as a function of grazing-incidence angle α for γ-Fe_2O_3 thin film. The critical angle of total reflection α_c is shown by the vertical arrows for different wavelengths.

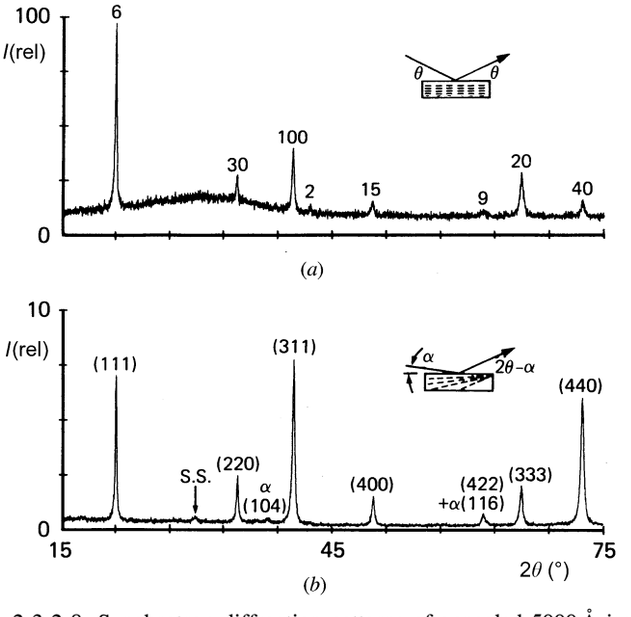

Fig. 2.3.2.8. Synchrotron diffraction patterns of annealed 5000 Å iron oxide film, $\lambda = 1.75$ Å, (*a*) θ–2θ scan; relative intensities of random powder sample shown above each reflection. (*b*) Grazing incidence pattern of same film with $\alpha = 0.25°$ showing only reflections from top 60 Å of film, superstructure peak S.S. and α-Fe_2O_3 peaks not seen in (*a*). Absolute intensity is an order of magnitude lower than (*a*).

dispersive diffraction (EDD) described in Section 2.5.1, the specimen and detector remain fixed at selected angles during the recording. This makes it possible to design special experiments that would not be possible with specimen-scanning methods. It also simplifies the design of specimen-environment chambers for high and low temperatures. The advantages of the method over conventional EDD are the order-of-magnitude higher resolution that can be controlled by the X-ray optics, the ability to handle high peak count rates with a high-speed scintillation counter and conventional circuits, and much lower count times for good statistical accuracy.

The accessible range of d's that can be recorded using a selected wavelength range is determined by the 2θ setting of the detector. Changing 2θ causes the separation of the peaks to expand or compress in a manner similar to a variation of λ in conventional diffractometry. This is illustrated in Figs. 2.3.2.9(*a*)–(*d*) for a quartz powder specimen using an Si(111) channel monochromator and $\theta_M = 19$ to 5° (2.04 to 0.55 Å, 6.1 to 22.7 keV) and four detector 2θ settings. At small 2θ settings, only the large d's are recorded and the peak separation is large. Increasing the 2θ setting decreases the d range and the separation of the peaks as shown in Fig. 2.3.2.9(*e*). These patterns were recorded with the pulse-height analyser set to discriminate only against scintillation counter noise.

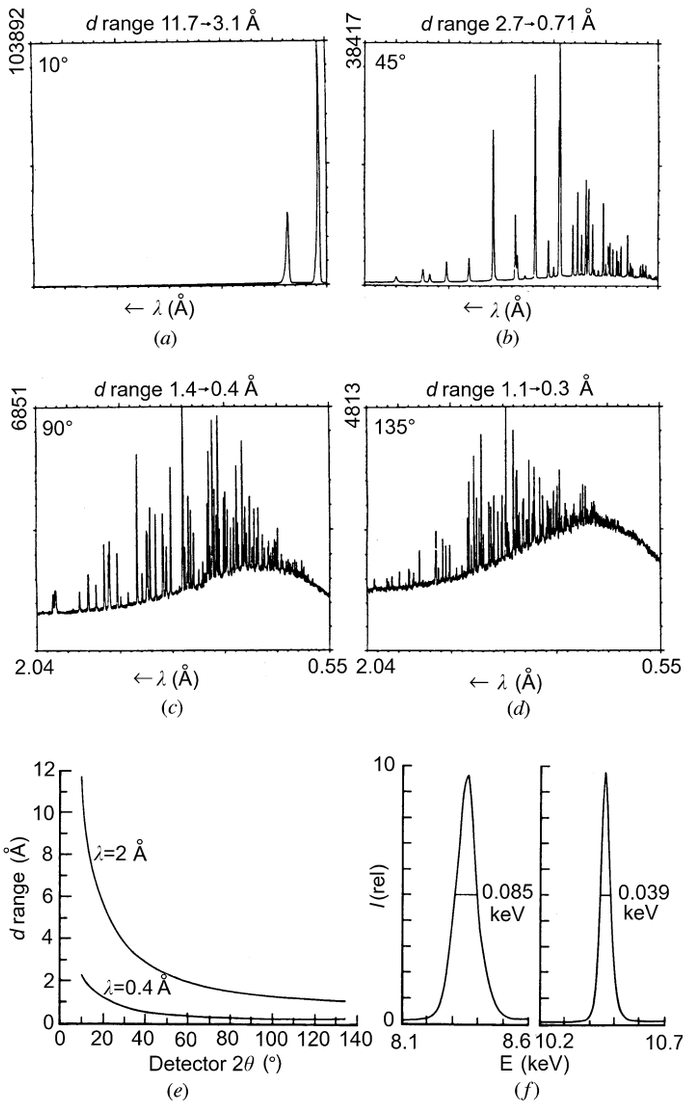

Fig. 2.3.2.9. (*a*)–(*d*) High-resolution energy-dispersive diffraction patterns of quartz powder sample obtained with 2θ settings shown in upper left corners. (*e*) d range as a function of detector 2θ setting for $\lambda = 0.4$ to 2 Å. (*f*) Effect of 2θ setting and E on profile widths of quartz. Right: 121 reflection, $20°2\theta$, E_p 10.45 keV; left: 100 reflection, $45°2\theta$, e_p 8.35; both reflections broadened by X-ray optics and peak intensity of 100 twice that of 121.

For given X-ray optics, the profiles symmetrically broaden with decreasing X-ray photon energy and with θ. This type of broadening remains symmetrical if E is increased and 2θ decreased, or *vice versa*, Fig. 2.3.2.9(*f*). The two profiles shown have been broadened by the X-ray optics but the intrinsic resolution is far better. The number of points recorded per profile thus decreases with decreasing profile width since $\Delta\theta_M$ is constant. At the higher energies, it may be desirable to use smaller $\Delta\theta_M$ steps to increase the number of points to define better the profile. Alternatively, increments in $\sin\theta$ steps rather than θ steps would eliminate this variation.

Many electronic solid-state devices use thin films that are purposely prepared to have single-crystal structure (*e.g.* epitaxic growth), or with a selected lattice plane oriented parallel or normal to the film surface to enhance certain properties. The properties vary with the degree of orientation and textural characterization is essential to make the correct film preparation. Preferred orientation can be detected by comparing the relative intensities of the thin-film pattern with those of a random powder. The pattern can be recorded with conventional θ–2θ scanning (λ fixed) or by EDD. However, this only gives information on the planes oriented parallel to the surface. To study inclined planes requires uncoupling the specimen surface and detector angles. This can be done with the EDD method described above without distorting the profiles (Hart *et al.*, 1987).

The principle of the method is illustrated in Fig. 2.3.2.10. The set of lattice planes (*hkl*) oriented parallel to the surface has its highest intensity in the symmetric θ–2θ position. Rotating the specimen by an angle θ_r while keeping 2θ fixed reduces the intensity of (*hkl*) and brings another set of planes (*pqr*), which are inclined to the surface, to its symmetrical reflecting position. The required rotation is determined by the interplanar angle between (*hkl*) and (*pqr*). The angular distribution of any plane can be measured with respect to the film surface by step scanning at small θ_r steps. The specimen is rotated clockwise with the limitation $\theta_s + \theta_r < 2\theta$. A computer automation program is desirable for large numbers of measurements.

Fig. 2.3.2.3(*c*) shows the appearance of a pattern of a specimen containing elements with absorption edges in the recording range and using electronic discrimination only against electronic noise. Starting at the incident high-energy side, the Zn and Ni K fluorescence increases as the energy approaches the edges (λ^3 law), decreases abruptly when the energy crosses each edge, and disappears beyond the Ni K edge. Long-wavelength fluorescence is absorbed in the windows and air path.

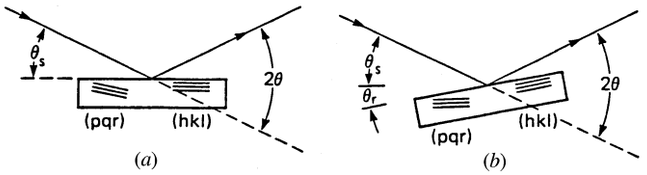

Fig. 2.3.2.10. Specimen orientation for symmetric reflection (*a*) from (*hkl*) planes and (*b*) specimen rotated θ_r for symmetric reflection from (*pqr*) planes.

The method is of doubtful use for structure determination or quantitative analysis. The wide range of wavelengths, continually varying absorption and profile widths, and other factors create a major difficulty in deriving accurate values of the relative intensities.

Conventional energy-dispersive diffraction methods using white X-rays and a solid-state detector are described in Chapter 2.5 and Section 5.2.7.

2.3.3. Specimen factors, angle, intensity, and profile-shape measurement

The basic experimental procedure in powder diffraction is the measurement of intensity as a function of scattering angle. The profile shapes and 2θ angles are derived from the observed intensities and hence the counting statistical accuracy has an important role. There is a wide range of precision requirements depending on the application and many factors are involved: instrument factors, counting statistics, profile shape, and particle-size statistics of the specimen. *The quality of the specimen preparation is often the most important factor in determining the precision of powder diffraction data.*

D. K. Smith and colleagues (see, for example, Borg & Smith, 1969; see also Yvon, Jeitschko & Parthé, 1977) developed a method for calculating theoretical powder patterns from well determined single-crystal structures and have made available a Fortran program (Smith, Nichols & Zolensky, 1983). This has important uses in powder diffraction studies because it provides reference data with correct I's and d's, free of sample defects, preferred orientation, statistical errors, and other factors. The data can be displayed as recorded patterns by using plot parameters corresponding to the experimental conditions (Subsection 2.3.3.9). Calculated patterns have been used in a large variety of studies such as identification standards, computing intermediate members of an isomorphous series, testing structure models, ordered and disordered structures, and others. Many experiments can be performed with simulated patterns to plan and guide research. The method must be used with some care because it is based on the small single crystal used in the crystal-structure determination and the large powder samples of minerals and ceramics, for example, may have a different composition. Errors in the structure analysis are magnified because the powder intensities are based on the squares of the structure factors.

The Lorentz and polarization factors for diffractometry geometry have been discussed by Ladell (1961) and Pike & Ladell (1961).

Smith & Snyder (1979) have developed a criterion for rating the quality of powder patterns; see also de Wolff (1968*a*).

2.3.3.1. *Specimen factors*

Ideally, the specimen should contain a large number of small equal-sized randomly oriented particles. The surface must be flat and smooth to avoid microabsorption effects, *i.e.* particle interferences which reduce the intensities of the incident and reflected beams and can lead to significant errors (Cline & Snyder, 1983). The specimen should be homogeneous, particularly if it is a mixture or if a standard has been added. Low packing density and specimen-surface displacement (§2.3.1.1.6) may cause significant errors. It is recommended that the powder and the prepared specimen be examined with a low-power binocular optical microscope. Smith & Barrett (1979), Jenkins, Fawcett, Smith, Visser, Morris & Frevel (1986), and Bish & Reynolds (1989) have surveyed methods of specimen preparation and they include bibliographies on special handling problems. Powder diffraction standards for angle and intensity calibration are described in Section 5.2.9.

2.3.3.1.1. *Preferred orientation*

Preferred orientation changes the relative intensities from those obtained with a randomly oriented powder sample. It occurs in materials that have good cleavage or a morphology that is platy, acicular or any special shape in which the particles tend to orient themselves in specimen preparation. The micas and clay minerals are examples of materials that exhibit very strong preferred orientation. When they are prepared as reflection specimens, the basal reflections dominate the pattern. It is common in prepared thin films where preferred orientation occurs frequently or may be purposely induced to enhance certain optical, electrical, or magnetic properties for electronic devices. By comparison of the relative intensities with the random powder pattern, the degree of preferred orientation can be observed.

Powder reflections take place from crystallites oriented in different ways in the instrument geometries as shown in Fig. 2.3.1.2. In reflection specimen geometry with θ–2θ scanning, reflections can occur only from lattice planes parallel to the surface and in the transmission mode they must be normal to the surface. In the Seemann–Bohlin and fixed specimen with 2θ scanning methods, the orientation varies from parallel to about 45° inclination to the surface. The effect of preferred orientation can be seen in diffraction patterns obtained by using the same specimen in the different geometries.

The effect is illustrated in Fig. 2.3.3.1 for *m*-chlorobenzoic acid, $C_7H_5ClO_2$, with reflection and transmission patterns and the pattern calculated from the crystal structure. The degree of preferred orientation is shown by comparing the peak intensities of four reflections in the three patterns:

(*hkl*)	(120)	(200)	(040)	(121)
Reflection	9.8	0.6	1.6	2.5
Transmission	5.2	0.5	0.7	9.3
Calculated	3.0	6.6	4.0	9.1.

Care is required to make certain the differences are not caused by a few fortuitously oriented large particles.

Various methods have been used to minimize preferred orientation in the specimen preparation (Calvert, Sirianni, Gainsford & Hubbard, 1983; Smith & Barrett, 1979; Jenkins *et al.*, 1986; Bish & Reynolds, 1989). These include using small particles, loading the powder from the back or side of the specimen holder, and cutting shallow grooves to roughen the surface. The powder has also been sifted directly on the surface of a microscope slide or single-crystal plate that has been wetted with the binder or petroleum jelly. Another method is to mix the powder with an inert amorphous powder such as Lindemann glass or rice starch, or add gum arabic, which after setting can be reground to obtain irregular particles. Any additive reduces the intensity and the peak-to-background ratio of the pattern. A promising method that requires a considerable amount of powder is to mix it with a binder and to use spray drying to encapsulate the particles into small spheres which are then used to prepare the specimen (Smith, Snyder & Brownell, 1979).

Preferred orientation would not cause a serious problem in routine identification providing the reference standard had a similar preferred orientation and both patterns were obtained with the same diffractometer geometry. However, when accurate values of the relative intensities are required, as in crystal-